

# Superlattice Structures in Morphologies of the ABC Triblock Copolymers

Yasuhiro Mogi,<sup>1a</sup> Mahito Nomura, Hiroyuki Kotsuji,<sup>1b</sup> Kouki Ohnishi,<sup>1c</sup> Yushu Matsushita,\* and Ichiro Noda

Department of Applied Chemistry, Nagoya University, Furo-cho, Chikusa-ku, Nagoya 464-01, Japan

Received November 30, 1993; Revised Manuscript Received July 20, 1994\*

**ABSTRACT:** Four types of morphologies, lamellar, ordered tricontinuous double-diamond (OTDD), cylindrical, and spherical structures, of isoprene (I)-styrene (S)-2-vinylpyridine (P) triblock copolymers having I and P block polymers with the same volume fractions, were studied by transmission electron microscopy (TEM) and small-angle X-ray scattering (SAXS). These studies revealed that the spherical structure has the packing manner of the CsCl type consisting of two spherical domains of I and P end-block polymers and the cylindrical structure, which consists of two kinds of cylindrical domains of end-block polymers, has the tetragonally-coarrayed pattern. Moreover, the OTDD structure proposed previously was confirmed by TEM observation of one (P domains) of the double-diamond frameworks in a film specimen stained with phosphotungstic acid. From these results, together with the TEM and SAXS studies on three-phase four-layer lamellar structure, we conclude that the morphologies of the triblock copolymers used in this work have the characteristics of superlattice structures.

## Introduction

The variation of morphology with composition has been extensively studied on AB diblock copolymers.<sup>2</sup> Recently, we studied the morphologies of microphase-separated structures of isoprene (I)-styrene (S)-2-vinylpyridine (P) triblock copolymers having I and P block polymers with the same volume fractions and found that the morphologies change in the order spherical, cylindrical, double-diamond, and lamellar structures, with decreasing the volume fraction of S block polymers similarly to IS diblock copolymers, though the composition range is different from that of IS diblock copolymers.<sup>3</sup> The variation of morphology of the triblock copolymers with composition can be explained by the theory of Nakazawa and Ohta.<sup>4</sup> Recently, it was reported by Gido et al. that a P-I-S triblock copolymer with a P/I/S volume ratio of 1/1/1 forms a peculiar morphology, which has a cylindrical core of P-domain surrounded by an annulus of I-domain within a matrix of S-domain.<sup>11</sup> However, we suppose that ABC triblock copolymers form symmetric equilibrium morphologies both when A and C blocks have the same volume fractions and when A/B and B/C interfaces possess similar surface energies if the system is in the strong segregation limit regime. In this work, therefore, we studied more in detail about the morphologies of ISP triblock copolymers having I and P block polymers with the same volume fractions by transmission electron microscopy (TEM) and small-angle X-ray scattering (SAXS).

## Experimental Section

ISP triblock copolymers used as samples were prepared by an anionic polymerization technique, and they were characterized as reported previously.<sup>3</sup> Their molecular characteristics are summarized in Table 1. Film specimens for TEM and SAXS were prepared by solvent-casting from 3 wt % tetrahydrofuran solutions and annealing *in vacuo* at 120 °C for 10 days. Morphologies of film specimens stained with OsO<sub>4</sub> or phosphotungstic acid (PTA) were observed with a transmission electron microscope (JEOL Model 2000 FX). SAXS measurements were performed with a Kratky U-slit camera (Anton Paar Co.), equipped with a step scanner and a scintillation counter, using

Table 1. Molecular Characteristics of ISP Triblock Copolymers and Their Morphologies in Bulk

sample code	$M_n \times 10^{-3}$	$M_w/M_n$	volume fraction			morphology
			I	S	P	
ISP-26	190	1.04	0.05	0.89	0.06	spherical
ISP-25	200	1.04	0.08	0.84	0.08	spherical
ISP-12	73	1.03	0.11	0.80	0.09	spherical
ISP-15	49	1.03	0.13	0.78	0.09	spherical
ISP-19	90	1.02	0.12	0.76	0.12	cylindrical
ISP-24	136	1.02	0.14	0.74	0.12	cylindrical
ISP-18	93	1.02	0.14	0.68	0.18	cylindrical
ISP-23	91	1.02	0.20	0.66	0.14	OTDD
ISP-14	64	1.04	0.22	0.59	0.19	OTDD
ISP-1	88	1.05	0.25	0.50	0.25	OTDD
ISP-3	100	1.05	0.26	0.48	0.26	OTDD
ISP-2	94	1.05	0.30	0.42	0.28	lamellar
ISP-5	58	1.04	0.32	0.35	0.33	lamellar
ISP-16	152	1.04	0.35	0.34	0.31	lamellar
ISP-4	61	1.04	0.36	0.31	0.33	lamellar
ISP-27	185	1.02	0.43	0.18	0.39	lamellar
ISP-28	170	1.01	0.47	0.08	0.45	lamellar

the Cu K $\alpha$  line of which the wavelength  $\lambda$  is 0.154 nm. The scattering intensities were measured in the  $x$ - $y$  plane when the primary beams are incident upon samples in the two directions ("through" or "edge" views) as shown in Figure 1. The SAXS data correction for slit smearing was carried out in the same manner as in a previous paper.<sup>3</sup> Details of all the experiments were described earlier.<sup>3,5,6</sup>

## Results

As reported previously,<sup>3</sup> four types of morphologies, which were not changed by annealing, are observed for ISP triblock copolymers having I and P block polymers with the same volume fractions as shown in Figure 2. In the electron micrographs of film specimens stained with OsO<sub>4</sub>, black, white, and gray images correspond to the I, S, and P domains, respectively. In the film specimens stained with PTA as shown in Figure 2d, on the other hand, only the P domain gives a black image, while the others are invisible.

Parts a and b of Figure 2 are micrographs of spherical and cylindrical structures, respectively. The former represents that the spherical structures consist of the two kinds (I and P) of spherical domains formed by the two end-block polymers in the S domain as a matrix, while the

\* Abstract published in *Advance ACS Abstracts*, September 15, 1994.

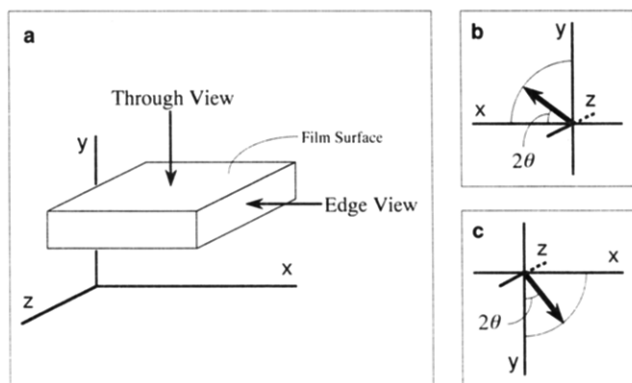


**Figure 1.** (a) Geometrical relationship between the incident beam and film specimen. The scattering angles,  $2\theta$ , for the two kinds of views are defined in each figure: (b) edge view; (c) through view.

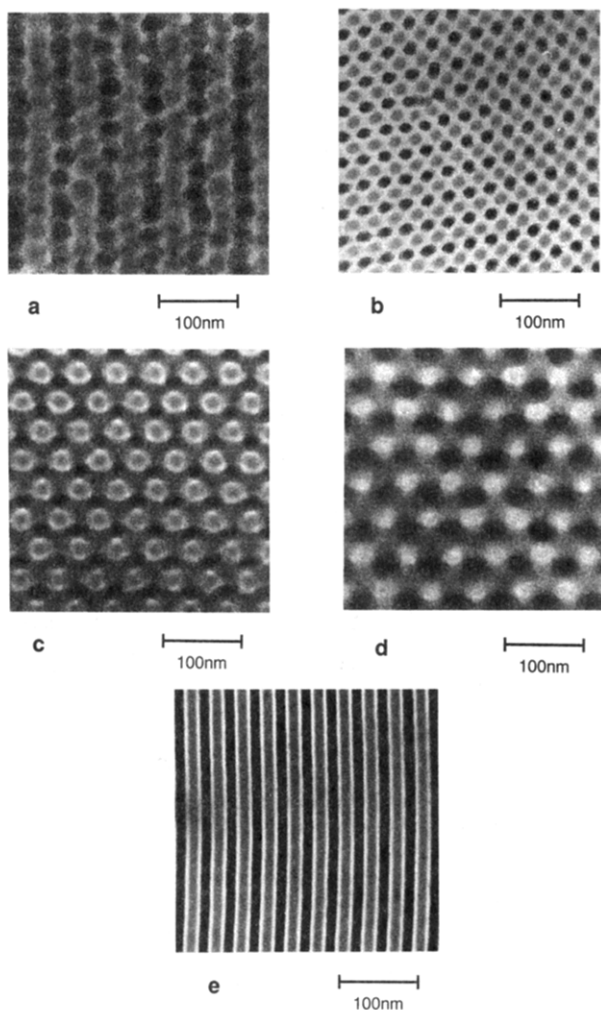


**Figure 2.** Typical examples of electron micrographs for four types of morphologies of microphase-separated structures of ISP triblock copolymers: (a) spherical structure (ISP-25); (b) cylindrical structure (ISP-19); (c and d) OTDD structure (ISP-3); (e) lamellar structure (ISP-4).

latter represents that the cylindrical structures consist of the two kinds (I and P) of cylindrical domains formed by the two end-block polymers in the S domain as a matrix. However, it is difficult to determine the types of packing for the spherical and cylindrical domains from these micrographs only.

Figure 3 is a triangle diagram demonstrating the variation of morphology with the composition of ISP triblock copolymers. Here two new data of ISP triblock

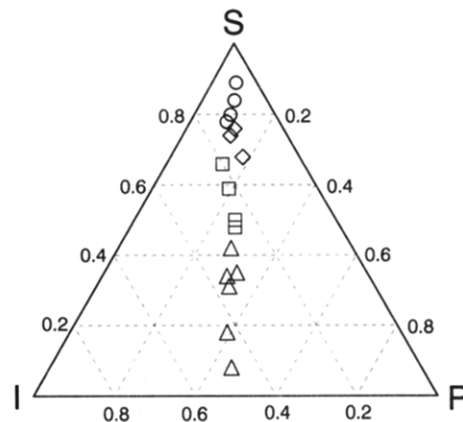


**Figure 3.** Triangle diagram demonstrating the variation of morphology with the volume fraction of the middle-block polymer in ISP triblock copolymers: spherical structure (O); cylindrical structure (◇); OTDD structure (□); lamellar structure (Δ).

copolymers with lower polystyrene contents were added to the previous one.<sup>3</sup> The new data indicate that the ISP triblock copolymers have lamellar structures, even when the volume fraction of polystyrene  $\Phi_S$  is lower than 0.3. This result implies that the ISP triblock copolymers may have lamellar structures in the range of  $\Phi_S$  from 0.42 down to 0, since IP diblock copolymers with the same volume fractions, which correspond to the ISP triblock copolymers with  $\Phi_S = 0$ , have lamellar structures.

Figure 4 shows semilogarithmic plots of SAXS intensity against the magnitude of scattering vector  $q$  ( $= (4\pi/\lambda) \sin \theta$ ) where  $2\theta$  is the scattering angle, for the spherical, cylindrical, ordered tricontinuous double-diamond (OTDD), and lamellar structures.

Figure 4a is a SAXS profile from the spherical structure of a ISP triblock copolymer. In this profile three diffraction peaks are observed at  $q_1 = 0.136$ ,  $q_2 = 0.240$ , and  $q_3 = 0.311 \text{ nm}^{-1}$ , respectively, and these give the ratios to be  $q_1/q_2 = 0.567$  and  $q_1/q_3 = 0.437$ . Apparently, these values are different from those of the diffraction patterns from the cubic close-packing for the spherical structures of diblock copolymers, of which the relative ratios of the diffraction peak positions should be  $q_1/q_2 = 1/\sqrt{2} = 0.707$  and  $q_1/q_3 = 1/\sqrt{3} = 0.577$ .<sup>7</sup>

Figure 4b is a SAXS profile from the cylindrical structure. In this figure, two diffraction peaks appear at  $q_1 = 0.147$  and  $q_2 = 0.332 \text{ nm}^{-1}$ , so that we have the ratio  $q_1/q_2 = 0.443$ . Obviously, this SAXS profile is different from that of the hexagonal close-packing for the cylindrical structures of diblock copolymers, of which the relative ratios of the diffraction peaks should be  $q_1/q_2 = 1/\sqrt{3} = 0.577$  and  $q_1/q_3 = 1/\sqrt{7} = 0.378$ .<sup>8</sup>

## Discussion

SAXS from microdomain structures may be generally described by a paracrystalline theory.<sup>9</sup> In this work, however, we are interested only in the  $q$  values for the diffraction peaks to determine the packing pattern in the microdomains, so that we first discuss the structure factor  $F(q)$  related to lattice structures in the scattering intensity  $I(q)$  given by

$$I(q) \propto |F(q)|^2 \quad (1)$$

and

$$F(q) = \sum_j f_j \exp(iq \cdot r_j) \quad (2)$$

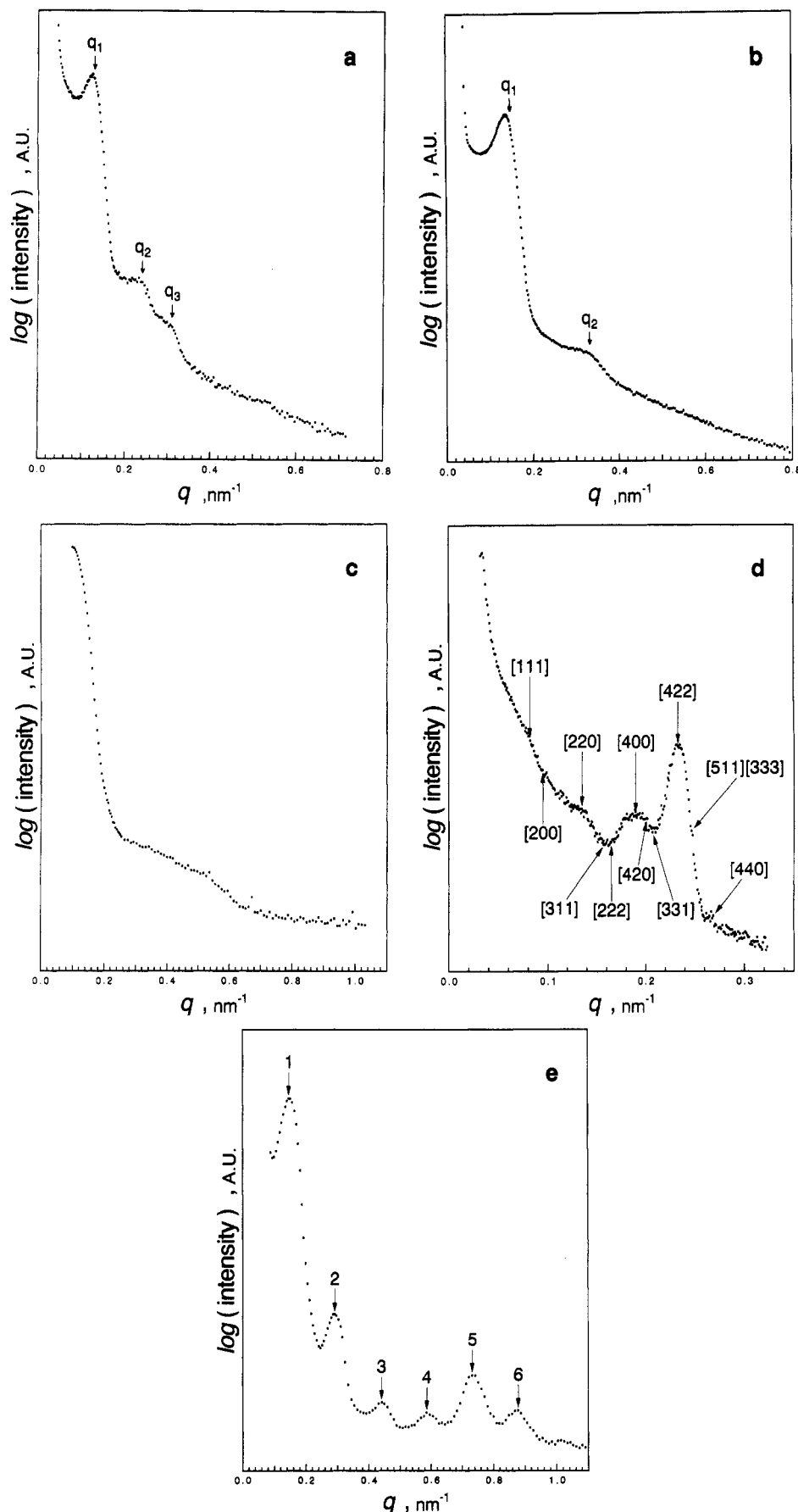


**Figure 4.** Examples of SAXS data for four types of morphologies of ISP triblock copolymers: (a) spherical structure (ISP-25); (b) cylindrical structure (ISP-18); (c) OTDD structure (ISP-1); (d) OTDD structure (ISP-20); (e) three-phase four-layer lamellar structure (ISP-5).

where  $j$  is the number signed to a scattering element in the unit cell,  $\mathbf{r}_j$  is the position vector of the  $j$ th scattering element, and  $f_j$  is its form factor determined by the electron

density, the volume, and the form of a microdomain, which is dependent on wave vector  $\mathbf{q}$  since the microdomain has a finite volume. Therefore, strictly speaking, it should be

**Table 2. Ratios of Intervals for the Diffraction Lattice Faces  $[hkl]$ 's to Those of the First Allowed Faces for Typical Packing Patterns of Structures with Two Kinds of Scattering Elements in Spherical and Cylindrical Morphologies**

packing patterns for two kinds of spheres						
CsCl ( $Fm\bar{3}m$ )	$[hkl]$	[100]	[111]	[210]	[221],[300]	[311]
	$d_{[hkl]}/d_{[100]}$	1	0.577	0.447	0.333	0.302
NaCl ( $Pm\bar{3}m$ )	$[hkl]$	[111]	[311]	[331]	[333],[511]	[531]
	$d_{[hkl]}/d_{[111]}$	1	0.522	0.378	0.333	0.293
sphalerite ZnS ( $F\bar{4}3m$ )	$[hkl]$	[111]	[200]	[311]	[222]	[331]
	$d_{[hkl]}/d_{[111]}$	1	0.866	0.522	0.500	0.378
WC $\alpha$ ( $P\bar{3}m1$ )	$[hkl]$	[100]	[101]	[111]	[102],[200]	[201]
	$d_{[hkl]}/d_{[100]}$	1	0.756	0.516	0.500	0.459
wurtzite ZnS ( $P6_3mc$ )	$[hkl]$	[100]	[101]	[110]	[102],[200]	[201]
	$d_{[hkl]}/d_{[100]}$	1	0.756	0.577	0.500	0.459
NiAs ( $P6_3/mmc$ )	$[hkl]$	[100]	[110]	[102],[200]	[112]	[202],[210]
	$d_{[hkl]}/d_{[100]}$	1	0.577	0.500	0.408	0.378
tetragonal packing for two kinds of cylinders	$[hkl]$	[100]	[210]	[300]	[320]	[410]
	$d_{[hkl]}/d_{[100]}$	1	0.447	0.333	0.277	0.243
hexagonal packing for two kinds of cylinders	$[hkl]$	[110]	[310]	[330]	[510]	[530]
	$d_{[hkl]}/d_{[110]}$	1	0.480	0.333	0.311	0.247

represented as  $f_j(\mathbf{q})$ . Since the electron density,  $\rho_j$ , can be assumed to be uniform in the microdomain, the form factor  $f_j$  is given by

$$f_j = \rho_j f'_j \quad (3)$$

where  $f'_j$  is the form factor free from the electron density value, which can be determined by the volume and the form of a microdomain only, and also is dependent on wave vector  $\mathbf{q}$ . Applying eq 2 to microdomain structures of ISP triblock copolymers and using eq 3, we have

$$\begin{aligned} F(\mathbf{q}) &= \sum f_I \exp(i\mathbf{q} \cdot \mathbf{r}_{jI}) + \sum f_S \exp(i\mathbf{q} \cdot \mathbf{r}_{jS}) + \sum f_P \exp(i\mathbf{q} \cdot \mathbf{r}_{jP}) \\ &= \rho_I f'_I \sum \exp(i\mathbf{q} \cdot \mathbf{r}_{jI}) + \rho_S f'_S \sum \exp(i\mathbf{q} \cdot \mathbf{r}_{jS}) + \rho_P f'_P \sum \exp(i\mathbf{q} \cdot \mathbf{r}_{jP}) \quad (4) \end{aligned}$$

where the subscripts I, S, and P denote I, S, and P domains, respectively. Moreover, we can rewrite eq 4 in terms of the difference between the electron densities of I or P domains and that of the S matrix domain as

$$\begin{aligned} F(\mathbf{q}) &= \Delta\rho_I f'_I \sum \exp(i\mathbf{q} \cdot \mathbf{r}_{jI}) + \Delta\rho_P f'_P \sum \exp(i\mathbf{q} \cdot \mathbf{r}_{jP}) + \\ &\quad \rho_S \{f'_I \sum \exp(i\mathbf{q} \cdot \mathbf{r}_{jI}) + f'_S \sum \exp(i\mathbf{q} \cdot \mathbf{r}_{jS}) + f'_P \sum \exp(i\mathbf{q} \cdot \mathbf{r}_{jP})\} \quad (5) \end{aligned}$$

where  $\Delta\rho_I = \rho_I - \rho_S$  and  $\Delta\rho_P = \rho_P - \rho_S$ . Since the third term denotes the structure factor for scattering from the unit cell having the uniform electron density of  $\rho_S$ , we can neglect this term in analyzing diffraction patterns. Using the Miller index of the diffraction lattice face,  $[hkl]$ , therefore, we have the structure factor of a unit cell for diffraction as

$$F(hkl) = f'_I \{\Delta\rho_I \sum \exp[2\pi i(x_j h + y_j k + z_j l)] + \Delta\rho_P \sum \exp[2\pi i(x_j h + y_j k + z_j l)]\} \quad (6)$$

where  $(x_j, y_j, z_j)$  are the coordinates of the  $j$ th scattering element. Here, we assumed the relation  $f'_I = f'_P$ , not only because the I and P block polymers have the same volume fractions but also because the I and P domains can be conceived to have the same form in the present ISP triblock copolymers. As a first approximation, moreover, we assume that  $\Delta\rho_I = -\Delta\rho_P$  since  $\Delta\rho_I = -0.289 \times 10^{23}$  (electrons/cm<sup>3</sup>) and  $\Delta\rho_P = 0.257 \times 10^{23}$  (electrons/cm<sup>3</sup>). Introducing this assumption into eq 6, we evaluated the relative ratios of intervals for diffraction lattice face  $[hkl]$ , i.e.,  $d_{[hkl]}$ 's to those of the first allowed faces for several

typical three-dimensional crystal lattices representing spherical structures and also for two two-dimensional crystal lattices representing cylindrical structures both consisting of the two kinds of scattering elements with the same numbers in the cell as listed in Table 2.

Comparison between the calculated  $d_{[hkl]}/d_{[100]}$  or  $d_{[hkl]}/d_{[111]}$  in Table 2 and the experimental results, i.e.,  $q_1/q_2 = 0.567$  and  $q_1/q_3 = 0.437$ , reveals that the packing manner of the CsCl type is the most probable one for the spherical structure of ISP-25. This crystal lattice consists of two sublattices of single cubic type where the element of one cubic lattice is located at the body-center of another cubic lattice. This structure is one of the simplest arrangements of two kinds of spherical elements in the three-dimensional space, so as to be adequate to the spherical structure of the ISP triblock copolymer having end-block polymers with the same volume fractions. It is to be noted that the domain spacing ( $D$ ) of spherical structure is 3 times as large as  $d_{[111]}$ , as shown in Figure 5a. Using  $q_2 = 2\pi/d_{[111]} = 0.240 \text{ nm}^{-1}$ , we obtained  $D = 78.5 \text{ nm}$  for ISP-25.

As for cylindrical domains we examine the hexagonal and tetragonal packings as shown in Figure 6, because the former is known as the packing manner for cylindrical structures of diblock copolymers and the latter is another probable type of symmetrical packing for two kinds of elements. Comparison between SAXS experimental data, i.e.,  $q_1/q_2 = 0.443$ , and calculated values listed in Table 2 reveals that the tetragonal packing manner is the more probable one for the cylindrical structure. Thus we call this morphology a "tetragonally-coarrayed cylindrical structure". The domain spacing  $D$  is twice as large as  $d_{[110]}$ , as shown in Figure 5b. Actually, however, it is evaluated by using  $D = 2^{1/2}d_{[100]}$  from the [100] diffraction because the diffraction from the [110] face does not appear in the SAXS profile according to the extinction rule. Using  $q_1 = 2\pi/d_{[100]} = 0.147 \text{ nm}^{-1}$ , we obtained  $D = 60.4 \text{ nm}$  for ISP-18. This value agrees reasonably well with the domain spacing (52 nm) obtained by TEM observation (see Figure 3 of ref 3).

In a typical SAXS profile from the OTDD structure a broad shoulder is observed as shown in Figure 4c. As shown in Figure 5c the unit cell of OTDD structure has the symmetry of the  $F\bar{4}3m$  space group, in which the first nine of the possible reflections are [111], [200], [220], [311], [222], [400], [420], [331], and [422], while that of OBDD has the symmetry of the  $Pn\bar{3}m$  space group, because two diamond framework domains are made of the same component, and in which a series of possible reflections is different from  $F\bar{4}3m$ . If a tetrapod unit can be regarded as a scattering element, the coordinates of two kinds of

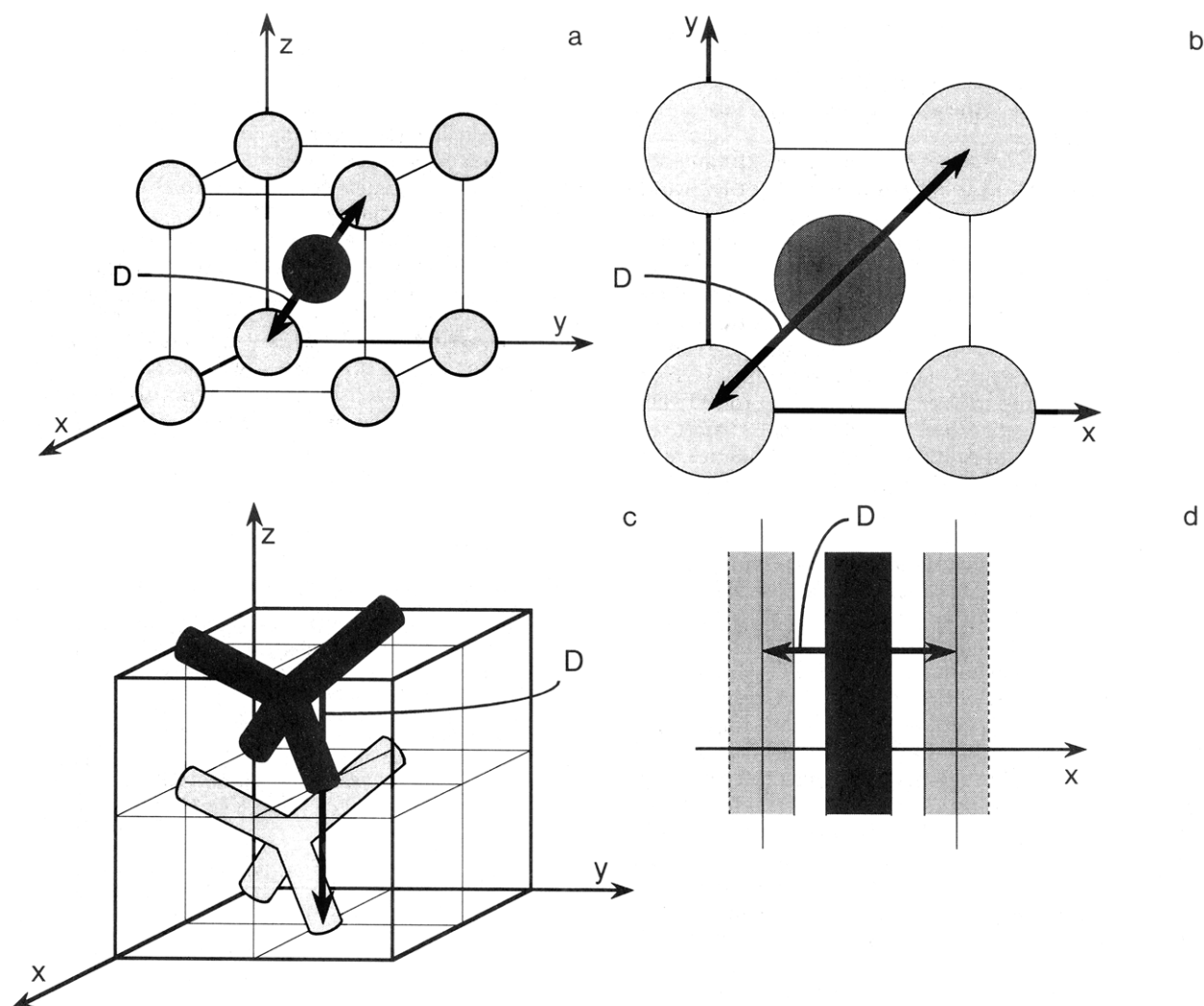


**Figure 5.** Unit cells and domain spacings for four types of morphologies of ISP triblock copolymers: (a) spherical structure; (b) cylindrical structure; (c) OTDD structure; (d) lamellar structure.

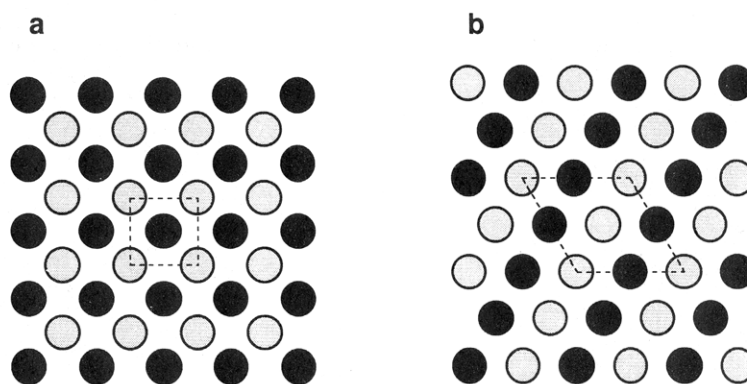


**Figure 6.** Schematic diagrams of two types of packing pattern for the cylindrical structures with two kinds of cylinders: (a) tetragonal packing; (b) hexagonal packing. The square and parallelogram drawn by the broken lines denote the unit cells for each packing.

tetrapods in a unit cell are given by

I-domain:  $(1/4, 1/4, 1/4), (1/4, 3/4, 3/4),$   
 $(3/4, 1/4, 3/4), (3/4, 3/4, 1/4)$

P-domain:  $(1/4, 1/4, 3/4), (1/4, 3/4, 1/4),$   
 $(3/4, 1/4, 1/4), (3/4, 3/4, 3/4)$

By applying these coordinates to eq 6, it is predicted that the reflections, whose sum of Miller indices,  $h + k + l$ , is odd, would be extinguished. It is to be noted that the SAXS data from OBDD structures were interpreted by

the same procedure, considering that the structure has the symmetry of  $Pn3m$ .<sup>12</sup> If the assumption  $\Delta\rho_I = -\Delta\rho_P$  is applied to the structure, moreover, the reflections whose three Miller indexes  $h, k$ , and  $l$  are all even may be extinguished. Consequently, all the reflections mentioned above disappear in the SAXS profiles from the OTDD structures. This prediction is almost satisfied except for the appearance of the broad shoulder as shown in Figure 4c. But this is not the case for a sample with low molecular weight. Figure 4d shows that several diffused peaks appeared in the relatively low  $q$  range which we were able to measure, and the peaks were assigned to the cor-

responding Miller indices. We consider that the predicted diffraction peaks may be shifted from a lower  $q$  range and became apparent because the size of a unit cell was small enough. The reason for the appearance of the peaks may be as follows.

The reflections, whose  $h + k + l$  is odd, are extinguished as expected as shown in this figure. On the other hand, the reflections for [220], [400], and [422] faces, whose three Miller indices are all even and  $h + k + l = 4n$ , where  $n$  is an integer, give the diffused peaks, though the reflections for [200], [222], and [420], whose Miller indices are all even but  $h + k + l = 4n - 2$ , are distinguished because of the extinction rule. These results may be caused by the fact that the deviation from the assumption  $\Delta\rho_I = -\Delta\rho_P$  is more magnified by the factor  $f'_I$  for OTDD structures than for spherical or cylindrical structures, because the volume fractions of end-block polymers in the former are larger than in the latter and also by the fact that a tetrapod cannot be regarded as a single scattering point.

Since it is not easy to confirm the morphology as the OTDD structure by SAXS as mentioned above, we studied the morphology by observing one of the double-diamond framework domains as well as both of them by TEM. Parts c and d of Figure 2 show micrographs of OTDD structure in film specimens stained with  $\text{OsO}_4$  and PTA, respectively. The former can be interpreted to be an image for a single layer consisting of a double-diamond framework of I and P domains as reported previously.<sup>4</sup> If this interpretation is valid, the latter must be an image for a single layer of a diamond framework of the P domain. This is the case, as is apparent from the comparison between Figure 2d and the image from the model for the OTDD structure in Figure 4 of a previous paper.<sup>5</sup> Thus we confirm that the structure consists of two kinds of diamond framework domains mutually interpenetrated, as sublattices.

Figure 4e shows a SAXS profile of three-phase four-layer lamellar structures where the diffraction peaks of integer-order are observed and the domain spacing can be evaluated by using the  $q_{\text{max}}$  from the [100] lattice face as shown in Figure 5d as reported previously.<sup>6</sup> Figure 2e shows a micrograph of the lamellar structure, which can

be regarded as a one-dimensional superlattice since the three kinds of lamellar domains are arranged in regular order in the structure.

In summary, we conclude that all the morphologies of ABC triblock copolymers having A and C block polymers with the same volume fractions possess the characteristics of superlattice structures if A/B and B/C interfaces have similar surface energies in the strong segregation limit regime. Thus, these triblock copolymers which have superlattice structures of various types in the order range of 10–100 nm will be useful for various applications.

**Acknowledgment.** This work was supported in part by a Grant-in-Aid for Scientific Research (No. 03750647) from the Ministry of Education and also supported by a grant from The Daiko Foundation. Y.M. is grateful for their support. The authors thank Mr. H. Choshi for his help in preparing samples and also in printing electron micrographs.

## References and Notes

- (1) Present address: (a) Idemitsu Petrochemical Co., Ltd., 1-1 Anesaki-Kaigan, Ichihara, Chiba, 299-01 Japan. (b) Nipponn Zeon Co., Ltd., 1-2-1 Yako, Kawasaki-ku, Kawasaki, 210 Japan. (c) School of Material Science, Japan Advanced Institute of Science and Technology, Hokuriku, Tatsuguchi-cho, Nomi-gun, Ishikawa, 923-12 Japan.
- (2) Molau, G. E. In *Block Polymers*; Aggarwal, S., Ed.; Plenum Press: New York, 1970.
- (3) Mogi, Y.; Kotsuji, H.; Kaneko, Y.; Mori, K.; Matsushita, Y.; Noda, I. *Macromolecules* **1992**, *25*, 5408.
- (4) Nakazawa, H.; Ohta, T. *Macromolecules* **1993**, *26*, 5503.
- (5) Mogi, Y.; Mori, K.; Matsushita, Y.; Noda, I. *Macromolecules* **1992**, *25*, 5412.
- (6) Mogi, Y.; Mori, K.; Kotsuji, H.; Matsushita, Y.; Noda, I. *Macromolecules* **1993**, *26*, 5169.
- (7) Hashimoto, T.; Fujimura, M.; Kawai, H. *Macromolecules* **1980**, *13*, 1660.
- (8) Richards, R. W.; Thomason, J. L. *Polymer* **1981**, *22*, 581.
- (9) Hosemann, R.; Bagchi, S. N. *Direct Analysis of Diffraction by Matter*; North-Holland: Amsterdam, The Netherlands, 1962.
- (10) Richards, R. W.; Thomason, J. L. *Macromolecules* **1983**, *16*, 982.
- (11) Gido, S. P.; Schwark, D. W.; Thomas, E. L.; Gonçalves, M. C. *Macromolecules* **1993**, *26*, 2636.
- (12) Thomas, E. L.; Alward, D. B.; Kinning, D. J.; Martin, D. C.; Handlin, D. L., Jr.; Fetters, L. J. *Macromolecules* **1986**, *19*, 2197.